



**HAL**  
open science

## Comparison of sunlight-AOPs for levofloxacin removal: kinetics, transformation products, and toxicity assay on *Escherichia coli* and *Micrococcus flavus*

Luca Foti, Donatella Coviello, Antonio Zuurro, Filomena Lelario, Sabino Aurelio Bufo, Laura Scrano, Andres Sauvêtre, Serge Chiron, Monica Brienza

### ► To cite this version:

Luca Foti, Donatella Coviello, Antonio Zuurro, Filomena Lelario, Sabino Aurelio Bufo, et al.. Comparison of sunlight-AOPs for levofloxacin removal: kinetics, transformation products, and toxicity assay on *Escherichia coli* and *Micrococcus flavus*. *Environmental Science and Pollution Research*, inPress, 10.1007/s11356-022-19768-w . hal-03648927

**HAL Id: hal-03648927**

**<https://imt-mines-ales.hal.science/hal-03648927>**

Submitted on 7 Jun 2022

**HAL** is a multi-disciplinary open access archive for the deposit and dissemination of scientific research documents, whether they are published or not. The documents may come from teaching and research institutions in France or abroad, or from public or private research centers.

L'archive ouverte pluridisciplinaire **HAL**, est destinée au dépôt et à la diffusion de documents scientifiques de niveau recherche, publiés ou non, émanant des établissements d'enseignement et de recherche français ou étrangers, des laboratoires publics ou privés.

# Comparison of sunlight-AOPs for levofloxacin removal: kinetics, transformation products, and toxicity assay on *Escherichia coli* and *Micrococcus flavus*

Luca Foti<sup>1</sup> · Donatella Coviello<sup>2</sup> · Antonio Zuorro<sup>3</sup> · Filomena Lelario<sup>1</sup> · Sabino Aurelio Bufo<sup>1,4</sup> · Laura Scrano<sup>5</sup> · Andrés Sauvetre<sup>6</sup> · Serge Chiron<sup>7</sup> · Monica Brienza<sup>1</sup>

## Abstract

Levofloxacin (LFX) is a widely used antibiotic medication. Persistent traces of LFX in water and wastewater may induce bacterial resistance. Photon-driven advanced oxidation processes (AOPs) can assist in attaining complete abatement of LFX for environmental protection. This work benchmarks different solar AOPs based on hydroxyl radical (OH<sup>•</sup>) and sulphate radical (SO<sub>4</sub><sup>•-</sup>) chemistry. Other oxidant precursors, as radical sources, were used to selectively control the generation of either hydroxyl radical (i.e., H<sub>2</sub>O<sub>2</sub>), sulphate radical (i.e., peroxydisulphate (PDS)), or a controlled mixture ratio of both OH<sup>•</sup>/SO<sub>4</sub><sup>•-</sup> (i.e., peroxymonosulphate (PMS)). The influence of pH on degradation performance was evaluated using unbuffered and buffered solutions. Simulated irradiation/PMS process exhibited a strong pH-dependence attaining partial degradation of ca. 56% at pH 5 up to complete degradation at pH 7. Despite the similitudes on the abatement of target pollutant LFX in pristine solutions, only simulated irradiation/PDS treatment achieved effective abatement of LFX in wastewater samples given the higher selectivity of SO<sub>4</sub><sup>•-</sup>. Toxicity tests were conducted with *Escherichia coli* (LMG2092) and *Micrococcus flavus* (DSM1790), demonstrating successful inhibition of the antibiotic character of polluted waters, which would contribute to preventing the development of resistant bacterial strains. Finally, a degradative pathway was suggested from the by-products and intermediates identified by LC–MS. Results demonstrate that the degradation of specific functional groups (i.e., piperazine ring) is associated with the loss of antibacterial character of the molecule.

**Keywords** Emerging contaminants · Levofloxacin · Photodegradation · AOPs · Toxicity · Sulphate radicals

## Abbreviations

AOPs	Advanced oxidation processes	PMS	Peroxymonosulphate
FQs	Fluoroquinolones	PDS	Peroxydisulphate
HR-AOPs	Hydroxyl radicals based advanced oxidation processes	SR-AOPs	Sulphate radicals-based advanced oxidation processes
LB	Lysogeny broth	TPs	Transformation products
LFX	Levofloxacin	TSB	Tryptic soy broth

Responsible Editor: Sami Rtimi

✉ Donatella Coviello  
coviello.donatella28@gmail.com

✉ Monica Brienza  
monica.brienza@unibas.it

<sup>1</sup> Department of Sciences, University of Basilicata, Via dell'Ateneo Lucano 10, 85100 Potenza, Italy

<sup>2</sup> Department of Engineering, University of Naples Parthenope, Centro Direzionale Isola C/4, 80143 Naples, Italy

<sup>3</sup> Department of Chemical Engineering, Materials & Environment, Sapienza University of Rome, Piazzale Aldo Moro 5, 00185 Rome, Italy

<sup>4</sup> Department of Geography, Environmental Management & Energy Studies, University of Johannesburg, Johannesburg 2092, South Africa

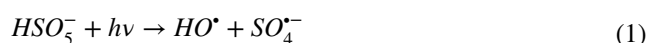
<sup>5</sup> Department of European and Mediterranean Cultures, University of Basilicata, Via Lanera 20, 75100 Matera, Italy

<sup>6</sup> UMR HydroSciences 5569, IMT Mines Alès, Montpellier Université, Montpellier, France

<sup>7</sup> Montpellier Université, UMR HydroSciences 5569, 15 Avenue Ch. Flahault, Montpellier cedex 5, 34093 Montpellier, France

Water pollution is an increasing environmental hot-spot due to the continuous introduction of recalcitrant organic compounds into the aquatic ecosystem (Geissen et al. 2015). Antibiotics are pharmaceuticals extensively used to treat and prevent bacterial infectious diseases. Despite being poorly regulated worldwide, antibiotics continue to be the most detected pharmaceuticals given their extensive use in human and veterinary medicine (Boy-Roura et al. 2018; Klein et al. 2018; Pascale et al. 2020). Effective removal of antibiotic trace levels from the environment is urgently required for a reason beyond the environmental impacts, such as toxicity to plants and other organisms (Backhaus et al. 2000; Mukhtar et al. 2020). Trace levels of antibiotics in aquatic ecosystems may induce the development of antibiotic resistance genes and bacteria, which will decrease or completely inhibit the therapeutic potential of antibiotics against human and animal pathogens (Rizzo et al. 2013; Zainab et al. 2020). This is a major risk for human health that should be prevented through effective antibiotic removal from the environment. The most detected classes of antibiotics in wastewater and surface water are fluoroquinolones (FQs) (Rizzo et al. 2013; Gothwal and Shashidhar 2015) because they are not removed in conventional wastewater treatment plants and can cause long-term bioaccumulation and toxicity in the environment (Liu et al. 2020). Usually, these fluorinated antibiotics are found at low concentrations, ranging from  $\text{ng L}^{-1}$  to  $\mu\text{g L}^{-1}$ , but concentrations up to several  $\text{mg L}^{-1}$  were already detected in effluents from pharmaceutical industries (Larsson et al. 2007). Fluoroquinolones are highly recalcitrant organic pollutants hardly removed by conventional water treatment technologies. The biodegradation of FQs has rarely been reported. To our knowledge, only a few bacteria (Pan et al. 2018) and fungi (Manasfi et al. 2020) species have been identified as organisms capable of biotransforming these antibiotic traces. However, the consequences due to the presence of fluoroquinolones in the environment are not fully understood, but they are known to be toxic to plants and aquatic organisms (Backhaus et al. 2000; Mukhtar et al. 2020). For this reason, the development of AOPs holds the promise of entirely mineralising pharmaceutical footprint in water environments if those are included as additional polishing to conventional wastewater treatment plants (Brienza and Katsoyiannis 2017). The fundamental principle of AOPs resides in the generation in situ of strong oxidising radical species such as hydroxyl radicals ( $\text{OH}^\bullet$ ), which interact with the molecules of the organic pollutants and lead to the progressive degradation of the contaminants (Lelario et al. 2016; Vagi and Petsas 2017). Hydroxyl radicals (HR) can be produced by different systems such as  $\text{UV}/\text{H}_2\text{O}_2$  (Jung et al. 2012),  $\text{UV}/\text{O}_3$  (Šojić et al. 2012),  $\text{UV}/\text{TiO}_2$  (Azzaz et al. 2018; Zuorro et al. 2019), Fenton, and photo-Fenton technologies (Kamagate et al. 2018; Zhu et al. 2019). In the

last decade, oxidants like persulphate ( $\text{PDS} = \text{S}_2\text{O}_8^{2-}$ ) or peroxymonosulphate ( $\text{PMS} = \text{HSO}_5^-$ ) have been studied as an alternative to conventional  $\text{OH}^\bullet$  based AOPs (Ahmed et al. 2014). In fact, through their activation, sulphate radicals ( $\text{SR})(\text{SO}_4^{\bullet-})$  can be produced for the removal of an extensive array of organic contaminants, including pharmaceuticals and pesticides (Kan et al. 2021). The activation of PMS and PDS can be achieved mainly by thermal, photolytic, sonolytic, radiolytic activation, and the reactions of the oxidants with iron oxide magnetic composites, including in situ formed iron hydroxides and quinones (Wacławek et al. 2017). Among the various SR-AOPs, sunlight technologies are desirable because of their low operational costs and high organic contaminants removal efficiency (Yang et al. 2019). After activation, PDS produces sulphate radicals, while PMS produces both sulphate and hydroxyl radicals, as reported in Eqs. 1–2:



Compared to  $\text{HO}^\bullet$ ,  $\text{SO}_4^{\bullet-}$  radicals have a series of advantages: higher redox potential ( $E^0 = 2.65\text{--}3.1$  V), higher selectivity and efficiency on the oxidation of compounds with unsaturated bonds or aromatic ring, higher pH range and higher half-life in some cases (Ahmed et al. 2012; Hayat et al. 2020). Therefore, sulphate radicals can remove emerging contaminants more efficiently (Wang and Wang 2018; Yang et al. 2019).

This work provides a framework to compare the effectiveness of homogeneous AOPs processes based on the generation of  $\text{OH}^\bullet$  and  $\text{SO}_4^{\bullet-}$  by solar-driven methods. Levofloxacin (LFX) is used as a model compound since it is the widest fluoroquinolone pharmaceutical and has been widely prescribed in the period of the COVID-19 pandemic due to its usefulness in the treatment of opportunistic bacterial infections that can co-occur during bacterial pathogenesis. In addition, the LFX transformation pathway has been investigated upon different oxidative treatments (Epold et al. 2015; Yahya et al. 2015) biodegradation (Shu et al. 2021), which might facilitate intermediates identification. The oxidants used are  $\text{H}_2\text{O}_2$ , PMS and PDS, which produce  $\text{HO}^\bullet$ ,  $\text{HO}^\bullet$ , and  $\text{SO}_4^{\bullet-}$ ,  $\text{SO}_4^{\bullet-}$  radicals respectively. In the first step, the performance of different AOPs was investigated in other pH conditions according to essential kinetic criteria, mainly the comparison between apparent first-order kinetic rate constants obtained by different SR-AOPs and HR-AOPs. Then, in a second step, treatment of LFX was conducted in a complex water matrix as representative wastewater composition to assess competitive and targeted reduction of fluoroquinolone at a realistic concentration level. To demonstrate the

hazard of the starting molecule and its degradation products, the evaluation of the inactivation of specific bacterial strains is beneficial (Cai et al. 2016). For this purpose, the effective inactivation of anti-bactericidal effects of LFX and by-products was evaluated using the culture of *Escherichia coli* and *Micrococcus flavus* microorganisms. The bactericidal effect evaluation is essential to define the effectiveness of technology to prevent the undesired development of bacteria-resistant strains.

## Material and methods

### Reagents, catalyst, and wastewater

For chemical analysis, acetonitrile (ACN) and formic acid were LC-MS grade from Honeywell (Wabash, IN, USA), and water was ultrapure Milli-Q grade (18.2 M $\Omega$  cm<sup>-1</sup> resistivity at 25 °C). Analytical standard of levofloxacin (LFX) (purity 99.4%) was purchased from Lab Instruments S.r.l. (Castellana Grotte, Puglia, Italy). Potassium peroxymonosulphate, with the commercial name of Oxone® (PMS, KHSO<sub>5</sub>·0.5KHSO<sub>4</sub>·0.5K<sub>2</sub>SO<sub>4</sub>), sodium persulphate (PDS, reagent grade, ≥98%), hydrogen peroxide (H<sub>2</sub>O<sub>2</sub>, 30%), potassium iodide (KI, ≥99.5%), sodium acetate trihydrate (CH<sub>3</sub>COONa·3H<sub>2</sub>O, ≥99%), monobasic potassium phosphate (KH<sub>2</sub>PO<sub>4</sub>, ≥99%), dibasic potassium phosphate (K<sub>2</sub>HPO<sub>4</sub>, ≥98%), sodium chloride (NaCl, ≥99.5%), calcium sulphate dihydrate (CaSO<sub>4</sub>·2H<sub>2</sub>O, ≥99%), magnesium sulphate (MgSO<sub>4</sub>, ≥97%), magnesium sulphate heptahydrate (MgSO<sub>4</sub>·7H<sub>2</sub>O, ≥98%), potassium chloride (KCl, ≥99%), urea (≥99.5%), peptone, yeast extract, agar, tryptone, and enzymatic digest of soybean meal were purchased from Sigma-Aldrich (St. Louis, USA), sodium hydrogen carbonate (NaHCO<sub>3</sub>, ≥99.5%) from VWR Chemicals (Radnor, PA, USA), glacial acetic acid (CH<sub>3</sub>COOH, ≥99.9%) and methanol (CH<sub>3</sub>OH, LC-MS grade) from Carlo Erba reagents (Milano, Italy), calcium chloride dihydrate (CaCl<sub>2</sub>·2H<sub>2</sub>O, ≥97%). All chemicals were used as received without further purification.

### AOPs and experimental conditions

The photocatalytic experiments were conducted using an amber cylindrical reactor covered with a quartz cap. The photochemical reactor was placed in a solar simulator device (Heraeus-Atlas Suntest CPS+, Chicago, USA), equipped with a Xenon Arc lamp (1.8 KW) as irradiation source, with a light power of 400 Wm<sup>-2</sup> and a spectral wavelength range of 290–800 nm. The temperature was kept constant (26 ± 0.1 °C) through an air conditioning system, and the solutions were maintained under continuous stirring to

ensure an optimum mixing flow. All photodegradation reactions were performed on a solution of LFX with an initial concentration of 10 mg L<sup>-1</sup>, obtained from a stock solution of 2000 mg L<sup>-1</sup> in methanol and diluted in different aqueous media: distilled water pH = 6.3, acetate buffer solution 0.01 M pH = 5, phosphate buffer solution 0.05 M pH = 7, simulated wastewater (SWW) pH = 7.8. The initial concentration was fixed at 10 mg L<sup>-1</sup> because it is suitable for kinetic competition experiments and allows HPLC quantification without pre-concentration steps. The efficiency of H<sub>2</sub>O<sub>2</sub>, PMS and PDS as oxidants at a concentration of 400 μM was assessed for each medium. Simulated wastewater (SWW) at pH around eight was employed in this work. The exact composition is as follows (Polo-López et al. 2012): NaHCO<sub>3</sub> (96 mg L<sup>-1</sup>), NaCl (7 mg L<sup>-1</sup>), CaSO<sub>4</sub>·2H<sub>2</sub>O (60 mg L<sup>-1</sup>), urea (6 mg L<sup>-1</sup>), MgSO<sub>4</sub> (60 mg L<sup>-1</sup>), KCl (4 mg L<sup>-1</sup>), K<sub>2</sub>HPO<sub>4</sub> (0.28 mg L<sup>-1</sup>), CaCl<sub>2</sub>·2H<sub>2</sub>O (4 mg L<sup>-1</sup>), peptone (32 mg L<sup>-1</sup>), and MgSO<sub>4</sub>·7H<sub>2</sub>O (2 mg L<sup>-1</sup>).

### Analytical methods

#### HPLC-UV and MS method for LFX analysis

The time course concentration of LFX was monitored using a high-performance liquid chromatography (HPLC) system (Agilent Technologies 1200 series, USA) equipped with a Kinetex C18 100 Å column (250 × 4.6 mm i.d. and 5 μm particle size) coupled to a diode array detector, set at λ = 295 nm. The mobile phase consists of a biphasic gradient, ultrapure water with 0.1% formic acid (solvent A) and acetonitrile (solvent B), structured as follows: 0–3 min, 0% B; 3–5 min, 15% B; 5–16 min, 15% B; 16–18 min, 100% B; 18–22 min, 100% B; 22–23 min, 0% B; 23–25 min, 0% B. The flow rate is 1.0 mL min<sup>-1</sup>, and the injection volume is 20 μL. The study of metabolites for LFX degradation in SWW by simulated irradiation/PDS was carried out using an LC-ESI(+)-linear trap quadrupole (LTQ) MS (Thermo Fisher Scientific, Bremen, Germany). Chromatographic conditions were maintained identical to those described above for the HPLC-UV method. The MS optimized experimental conditions for the ESI ion source were: ESI needle voltage, +4.5 kV; cone voltage, +3.00 kV; the temperature of the heated capillary, 350 °C; and sheath gas (N<sub>2</sub>) flow rate of 60 arbitrary units (a.u.). The instrument was externally calibrated with appropriate standards, and mass spectrometric data were acquired in the positive ion mode while scanning m/z 50–2000.

#### Spectrophotometric method for PDS quantification

During degradation, residual PDS concentration in SWW samples was monitored using a UV/visible single-ray

spectrophotometer Cary 50 at  $\lambda=352$  nm and  $\lambda=400$  nm. The analyzed solutions consisted of 1 mL of the selected sample, 1 mL of  $\text{NaHCO}_3$   $5.0$  mg  $\text{mL}^{-1}$ , 1 mL of KI  $0.1$  g  $\text{mL}^{-1}$ . Samples were maintained under dark conditions for 15 min and then placed into the spectrophotometer for analysis (Liang et al. 2008).

### Antibacterial activity assessment

The antibacterial effect of treated solutions was assessed on *E. coli* (LMG2092) and *M. flavus* (DSM1790). These analyses aimed to quantify the effective inhibition of antibacterial character to the effluent to prevent the development of antibiotic-resistant strains. Therefore, studies were carried out by testing the samples obtained from photodegradation experiments of LFX in SWW with simulated irradiation/PDS. Tryptic soy broth (TSB) and lysogeny broth (LB) were used as agar medium. TSB was prepared to dissolve 15.0 g tryptone, 5.0 g enzymatic digest of soybean meal, 5.0 g sodium chloride, 15.0 g agar in 1 L of distilled water. In comparison, LB medium was made up of 10.0 g peptone, 5.0 g yeast extract, 5.0 g sodium chloride and 12.0 g agar in 1 L of distilled water. Both the mediums were sterilized in a high-pressure sterilizer at  $121$  °C for 15 min and deposited into Petri dishes with a diameter of 60 mm (MacWilliams and Liao 2006). The suspensions of *E. coli* and *M. flavus* bacteria were prepared to contain approximately  $10^8$  CFU  $\text{mL}^{-1}$ . Each Petri dish was spiked in four different points with  $20$   $\mu\text{L}$  of four different samples, then finally incubated at a temperature of  $37$  °C for 18 h.

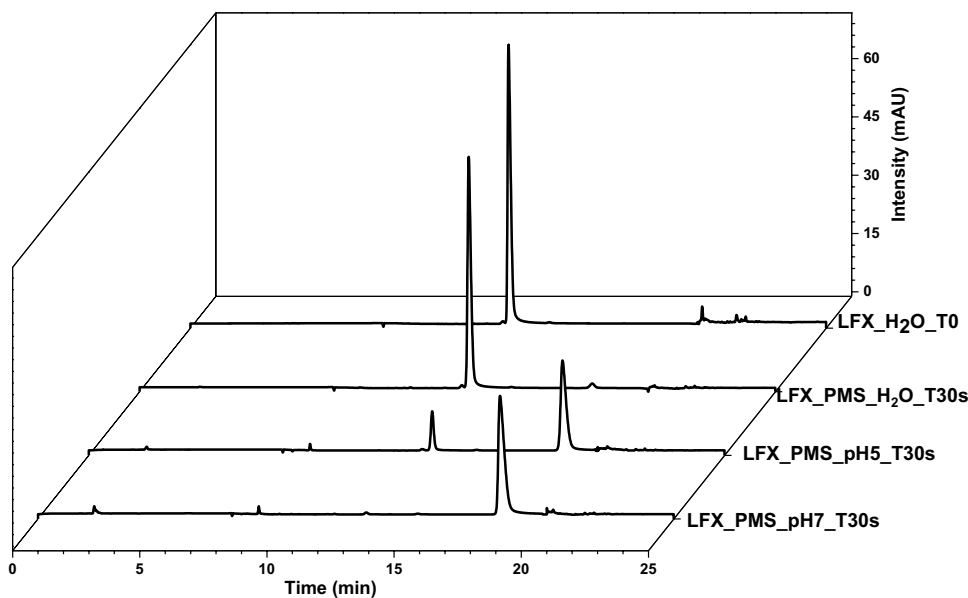
## Results and discussion

### Degradation efficiency of levofloxacin by simulated irradiation-drive processes

Before undertaking the LFX photodegradation studies in distilled water, acetate buffer, and phosphate buffer, a control experiment was carried out under dark conditions with an initial concentration of LFX at  $10$  mg  $\text{L}^{-1}$ , with and without  $\text{H}_2\text{O}_2$ , PMS and PDS. In these conditions, there was no evidence for LFX degradation in the presence of  $\text{H}_2\text{O}_2$ . As far as PDS is concerned, a decrease in the percentage of degradation is observed with increasing pH, except distilled water, which has a zero-degradation rate. Finally, concerning PMS, there is an increase in the degradation percentage as the pH increases, except for distilled water again. This anomalous behavior in distilled water could be attributed to the absence of ions in the solution. In particular, after 30 s adding of PDS, we obtained a decrease of 1%, 17%, and 10% in LFX concentration, while after adding PMS, we obtained a reduction of 10%, 40%, and 100% in distilled water, acetate buffer and phosphate buffer, respectively. In the case of PMS in phosphate buffer solution, we observe a complete transformation of LFX in just 30 s, as shown in the chromatogram of Fig. 1.

All the LFX (retention time 13.3 min) was transformed into another compound with a retention time of 18.4 min. This was identified as LFX N-oxide (Merel et al. 2017). Indeed, as reported for other fluoroquinolone antibiotics and nitrogenous heterocyclic compounds (Brienza et al. 2019, 2020; Nihemaiti et al. 2020), especially PMS can degrade organic contaminants without radicals involvement through

**Fig. 1** Chromatograms of LFX  $10$  mg  $\text{L}^{-1}$  in distilled water and after adding PMS [ $400$   $\mu\text{M}$ ] in distilled water, acetate buffer solution pH=5 and phosphate buffer solution pH=7



an oxidation process, and it has been demonstrated that the piperazine ring is the leading reaction site for quinolone compounds. This mechanism is still little studied, but it is closely related to the range of pH used in the experimental setup and seems to be improved in alkaline conditions (Wang and Wang 2018).

To compare the efficiency of sunlight-driven advanced oxidation processes, a kinetic study of LFX photodegradation using different oxidant systems such as H<sub>2</sub>O<sub>2</sub>, PMS, and PDS and represented by the following reactions in Eqs. 3–5 was carried out, and the results obtained were reported in Table 1:



From the results obtained, minimal degradation is observed during photolysis processes and in the presence of H<sub>2</sub>O<sub>2</sub>; meanwhile, high percentage degradation in a range of 25 to 100 and 89.2 to 100% was observed by PMS and PDS, respectively. This result can be explained by the small yield of OH<sup>•</sup> induced by simulated irradiation. It is important to remark that photolysis of H<sub>2</sub>O<sub>2</sub> from reaction (1) only takes place under UVC wavelengths. The spectrum of solar radiation has a small component of UV-light (<4.0%), from which UVC represents an almost null percentage (Serrà et al. 2021). Therefore, it cannot be expected a high efficiency in the photoactivation of H<sub>2</sub>O<sub>2</sub> to produce a high concentration of OH<sup>•</sup> for LFX degradation.

In the case of PDS, there is an increase of degradation rate when switching from acetate buffer solution pH 5 to distilled water pH 6.3 and a decrease when switching to phosphate buffer pH 7. At the same time, for H<sub>2</sub>O<sub>2</sub>, there is a continuous increase when changing from acidic to neutral pH, in agreement with the results reported by Lau et al. (2007) and Liu et al. (2013). There are some main reasons for this observed behavior: (i) the increase of pH in the solution

determines a different degree of molecule protonation, which will therefore have a distinct affinity for the radicals present; moreover, (ii) the more or less acidic aqueous environment may determine an abundant production of radicals, which results in a different number of degraded molecules depending on their total concentration. Furthermore, all the variations occurring in a solution determine a different degree of light absorption and, therefore, an extra degradation efficiency (Lau et al. 2007; Liu et al. 2013).

The kinetics of degradation of the various oxidants at different pH under simulated irradiation conditions are shown in Fig. 2.

Under photolysis and simulated irradiation/H<sub>2</sub>O<sub>2</sub> system, we have linear one-step degradation kinetics in all the solutions tested. In contrast, for simulated irradiation/PDS and affected irradiation/PMS systems, we have a first step where there is a rapid decrease in the concentration of the LFX due to a possible direct and immediate action of the oxidants adding and depending on the pH of the solutions tested, as said above, followed by a second step where we have a much slower degradation. However, the effect of pH value in the simulated irradiation/PDS process was smaller than that in the simulated irradiation/PMS process. In all cases, the first process led to complete degradation of LFX in 10 min and 20 min for distilled water and acetate/phosphate-buffered solutions, respectively.

Beyond direct comparison between the different reactions of AOPs, the simulated radiation activates the oxidants, resulting in hydroxyl and sulphate radicals forming depending on the chemical nature of the oxidants (Eq. 3 and Eq. 5). However, the results obtained indicate that SO<sub>4</sub><sup>•-</sup> radicals are more reactive towards the molecule of LFX concerning OH<sup>•</sup> radicals (Brienza et al. 2014). These results also demonstrate that, in this specific case, the activation of PDS through the use of only simulated radiation is sufficient to degrade LFX at a concentration of 10 mg L<sup>-1</sup>. However, in literature, most researchers focus on the metal-induced activation of PDS using metal ions such as Cu<sup>2+</sup>, Fe<sup>2+</sup>, Zn<sup>2+</sup>, or Mn<sup>2+</sup> (Wang et al. 2018; Gao and Zou 2020; Liu et al. 2021).

### Kinetic study of simulated irradiation/PDS system in simulated wastewater (SWW) and optimization of the process

Wastewater matrices present a complex composition that may affect the overall treatment performance of a treatment technology due to the existence of competitive species that may consume radicals produced (Garcia-Segura et al. 2020). Although methanol is an excellent scavenger for hydroxyl radicals (Bartlett and Cotman 1949; Jiménez et al. 2003), in our case, the small amount of methanol was considered part of the complex and its influence in this scenario was not significant. Given the high performance of the simulated

**Table 1** Percentage (%) of LFX degraded in acetate buffer solution, distilled water and phosphate buffer solution by different simulated irradiation/oxidant systems (*t* = 10 min)

	% Photodegradation		
	Acetate buffer solution (pH=5)	Distilled water (pH=6.3)	Phosphate buffer solution (pH=7)
Photolysis	3.0	2.5	13.9
H <sub>2</sub> O <sub>2</sub>	8.0	6.8	17.2
PMS	52.5	25.0	100.0
PDS	92.8	100.0	89.2

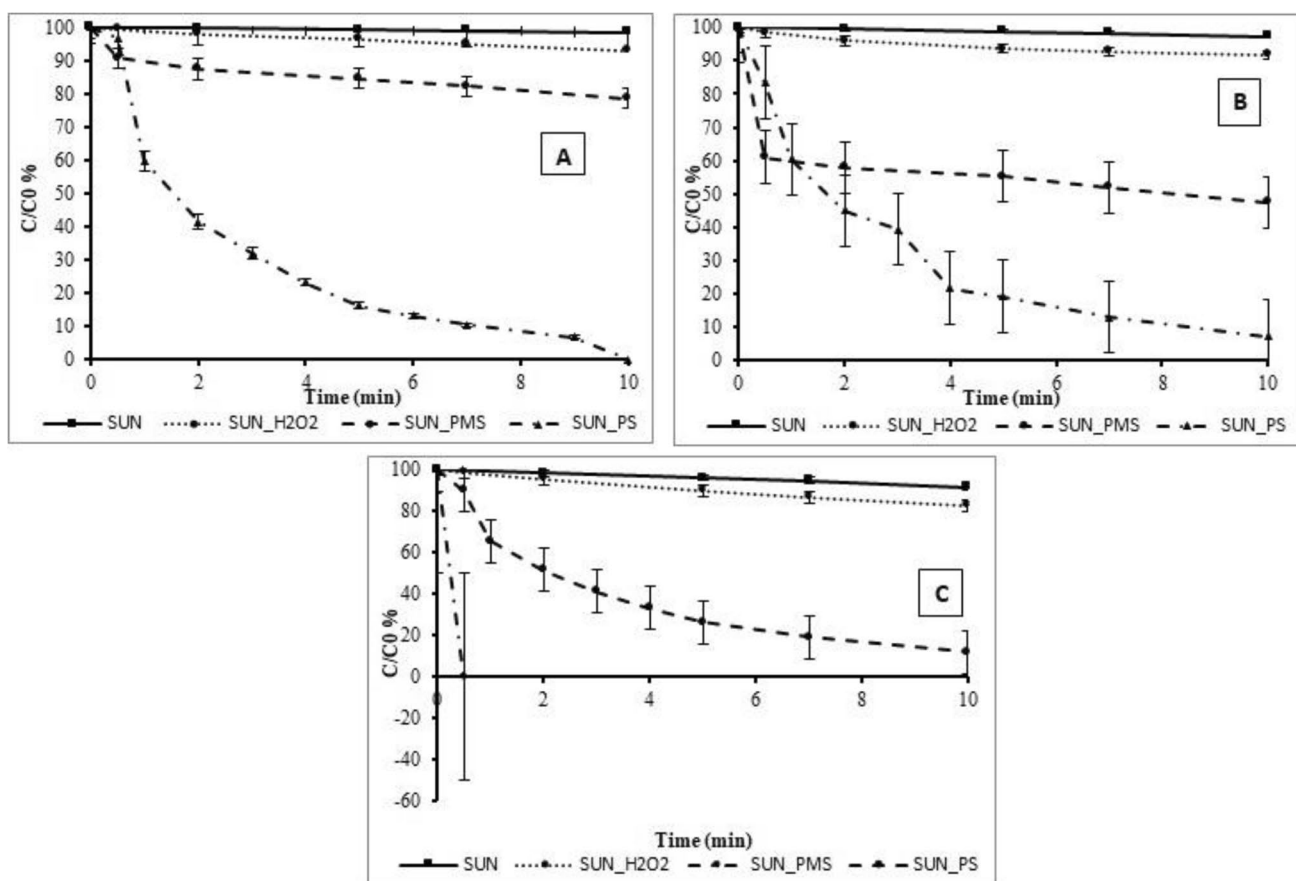


**Fig. 2** Photodegradation curve of LFX in **A** distilled water **B** acetate buffer solution, and **C** phosphate buffer solution, by different simulated irradiation/oxidant system ( $t = 10$  min;  $C_0 = 10$  mg L<sup>-1</sup>)

irradiation/PDS treatment, this process was selected to conduct further studies in a complex wastewater sample. Due to the ongoing COVID-19 pandemic, it was impossible to use an accurate wastewater sample for safety reasons; therefore, we used simulated wastewater, according to Polo-López et al. (2012). It can be observed that, despite the complex composition, the simulated irradiation/PDS treatment attains complete degradation of target LFX in 10 min with 400  $\mu$ M PDS dose. The remaining PDS in the solution was quantified through spectrophotometric analyses (Liang et al. 2008). A remaining concentration of 275  $\mu$ M PDS was quantified after treatment, suggesting that only 125  $\mu$ M PDS was required to attain complete abatement of LFX. Dose optimization is crucial to minimize capital expenditures and decrease risks associated with unwanted remaining concentrations of oxidants in treated water effluents. Additional experiences were conducted using lower initial doses of PDS of 100  $\mu$ M and 200  $\mu$ M (Fig. 3).

In Fig. 3, it can be seen that all three concentrations achieved almost complete degradation of LFX. Considering 10 min of residence time, LFX removal reached 86.4%, 93.1%, and 100% for increasing doses of PDS of 100  $\mu$ M,

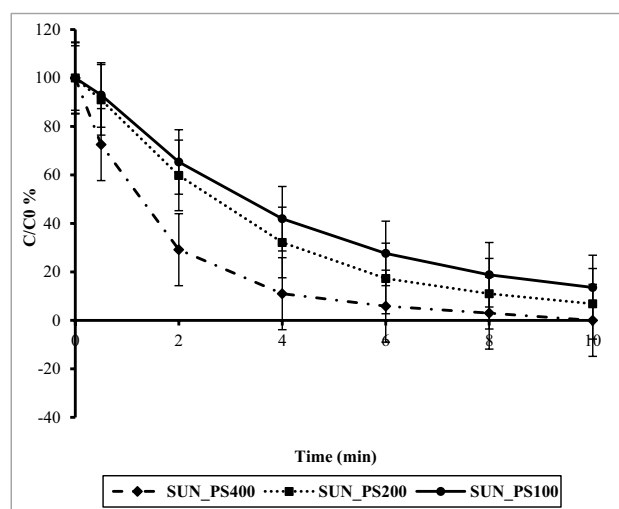


**Fig. 3** Kinetics degradation by simulated irradiation/PDS system at different PDS concentrations [400  $\mu$ M; 200  $\mu$ M; 100  $\mu$ M] in simulated wastewater (pH = 7.8;  $t = 10$  min;  $C_0 = 10$  mg L<sup>-1</sup>)

200  $\mu\text{M}$ , and 400  $\mu\text{M}$ , respectively. Thus, it can be observed that a lower amount of 200  $\mu\text{M}$  can be used to attain one log removal of trace pollutant LFX in wastewater samples. All normalized concentration of LFX was fitted according to a simple first-order kinetic model (Fig. 4) described by Eq. 6. The kinetic rate constant ( $k$  ( $\text{min}^{-1}$ )) and the corresponding half-reaction time (Eq. 7) (Table 2) were determined to find the best fit between the experimental and the calculated concentration of LFX profiles obtained with the simulated irradiation/PDS system.

$$\ln([A_0]) = -kt \quad (6)$$

$$t_{1/2} = \frac{\ln(2)}{k} \quad (7)$$

Figure 4 indicates that a decrease in initial oxidant dose slowed the kinetics of LFX abatement. The kinetic analysis shows pseudo-first-order rate constants ( $k_f$ ) of  $4.261 \times 10^{-1} \text{ min}^{-1}$  ( $R^2=0.993$ ) for 400  $\mu\text{M}$ ,  $2.726 \times 10^{-1}$  ( $R^2=0.996$ ) for 200  $\mu\text{M}$ ,  $2.019 \times 10^{-1} \text{ min}^{-1}$  ( $R^2=0.997$ ) for 100  $\mu\text{M}$ . The faster decrease observed in the wastewater concerning ultrapure water suggests that some components may facilitate the degradation of LFX. The decrease in  $k_f$  with decreasing dose of PDS can be explained by the lower yield when decreasing the concentration of precursor, which would

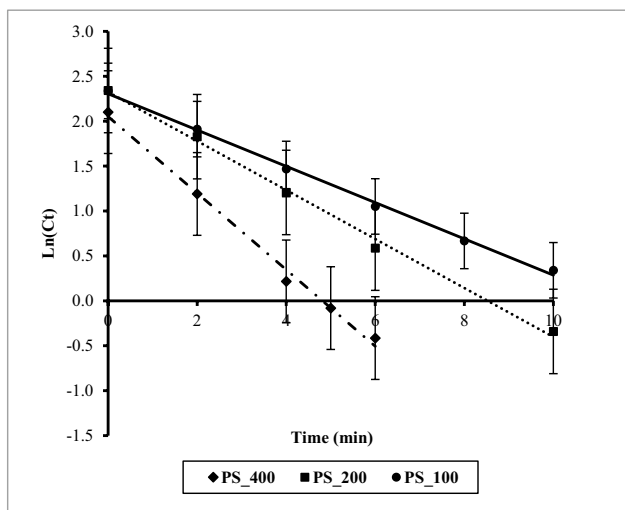


**Fig. 4** Trends of first-order linearized equation used for the calculation of kinetic parameters reported in Table 2

**Table 2** Kinetic parameters of LFX degradation in synthetic wastewater with three different concentrations of PDS

System	$(C_{\text{exp}} - C_{\text{calc}})^2$	$R^2$	$t_{1/2}$ (min)	$k$ ( $\text{min}^{-1}$ )
Simulated irradiation/PDS_100	0.1584	0.9975	3.43	0.2019
Simulated irradiation/PDS_200	0.1125	0.9960	2.54	0.2726
Simulated irradiation/PDS_400	0.1025	0.9934	1.63	0.4261

decrease the availability of oxidant to react with the same concentration of target pollutant LFX.

### Antibacterial activity (*E. coli* and *M. flavus*)

The LFX molecule contains several active functional groups that have been demonstrated to effectively induce toxicity to microorganisms in an aqueous ecosystem. Those vibrant centers are responsible for the antibacterial activity of LFX that is used to treat both Gram-negative and Gram-positive bacterial infections. Trace concentration levels of antibacterial pharmaceuticals in water samples below the lethal dose for bacteria ( $\text{LD}_{50}$ ) can cause the proliferation of multi-resistant strains. This analysis aims to evaluate the successful inhibition of the antibacterial activity of LFX and by-products to demonstrate that simulated irradiation/PDS can be an effective treatment technology to remove LFX and prevent the development of bacteria strains resistant to antibacterial drugs. Therefore, an antibacterial activity test was performed against Gram-negative *E. coli* (LMG2092) in the TSB medium and Gram-positive *M. flavus* (DSM1790) in the LB medium. The toxicity results were expressed by measuring the diameter of the culture inhibition halo.

Blank experiments were conducted before the antibacterial activity assessment on the samples obtained during the simulated irradiation/PDS treatment to evaluate the potential toxicity of PDS, methanol, and simulated wastewater. The results obtained showed that none of the tested concentrations of PDS (50  $\mu\text{M}$  ÷ 400  $\mu\text{M}$ ), methanol and SWW had any inhibition activity on the tested bacteria. Based on these results, it was also possible to test the mix of LFX transformation products in SWW with PDS.

The samples tested were the solution containing LFX 10  $\text{mg L}^{-1}$  in SWW ( $t_0$ ) and the solutions obtained after 5, 10, 30, 60, and 120 min of irradiation in the presence of PDS. The results obtained from the first sample ( $t_0$ ) analysis showed a growth inhibition halo with a diameter of 19 mm and 20 mm for *E. coli* and *M. flavus*, respectively, thus demonstrating the toxicity of LFX. In subsequent analysis after 5 min of treatment, we observed a notorious decrease in the inhibition halo on *E. coli* down to a diameter of 10 mm, almost 50% decrease in diameter. Meanwhile, no halo was observed for *M. flavus*, suggesting that after 5 min of treatment, there is no remaining antibacterial activity for Gram-positive microorganisms. Any halo was observed in the other samples tested on *E. coli* and *M. flavus*. The decrease in the antibacterial activity may

be attributed to the breaking down of the molecular structure and the elimination of some functional groups (quinolonic ring and piperazine ring) responsible for the toxicity of quinolone antibiotics thanks to the binding with DNA gyrase enzyme. The DNA gyrase is an essential bacterial enzyme that allows the replication of DNA (Chu and Fernandest 1989). Furthermore, it has been reported that some moieties, such as piperazine, carboxylic acid and keto groups in quinolones molecules, played essential roles in killing Gram-positive bacteria (Neth et al. 2019). The toxicity studies demonstrate the effectiveness of simulated irradiation/PDS treatment to completely degrade the functional groups of LFX and its degradation by-products associated with the antibacterial character of the pharmaceutical (Li et al. 2015; Zhou et al. 2021). These promising results suggest that simulated irradiation/PDS treatment might be a feasible solution to prevent the undesired release of trace antibacterial fluoroquinolone pharmaceuticals to the environment.

### Elucidation on degradation pathways of levofloxacin

The toxicity analyses allow inferring the degradation of different functional groups with antibacterial effects such as the piperazine ring. To elucidate the possible degradation pathway of LFX induced by simulated irradiation/PDS, aliquots were analyzed by the HPLC–MS to identify intermediates and by-products yielded from the radical-mediated oxidation. Structure analysis of the main degradation products was based on literature and fragmentation data obtained by positive ion collision dissociation (data not shown). In Fig. 5, the structure and the  $m/z$  ratio of all photo-products detected as  $[M + H]^+$  ions and the proposed degradation pathway are reported.

The parent compound LFX exhibits as  $[M + H]^+$  ion a nominal  $m/z$  ratio of 362 and, as highlighted in Fig. 5, undergoes further losses and substitutions forming, directly, eight main photoproducts. These primary products were themselves degraded, and we observed a quick increase during the first minutes and then a rapid decrease. After 10 min, the concentrations of LFX and all by-products identified were below the LOD, suggesting the complete disappearance of aromatic structures. The breakage of aromatic rings is commonly reported for other AOPs resulting in the yield of biodegradable carboxylic acids of low molecular weight (e.g., oxalic acid, oxamic acid, formic acid). The classification of identified by-products allows depicting different organic events of relevance that justify the loss of the antibacterial character of the effluent. As described above, certain functional groups are associated with toxic effects on Gram-positive and Gram-negative bacteria. These results agree with the previous discussion and suggest the competitive degradation of LFX and effective inactivation of the antibacterial character of the effluent. Identifying stable intermediates presents the

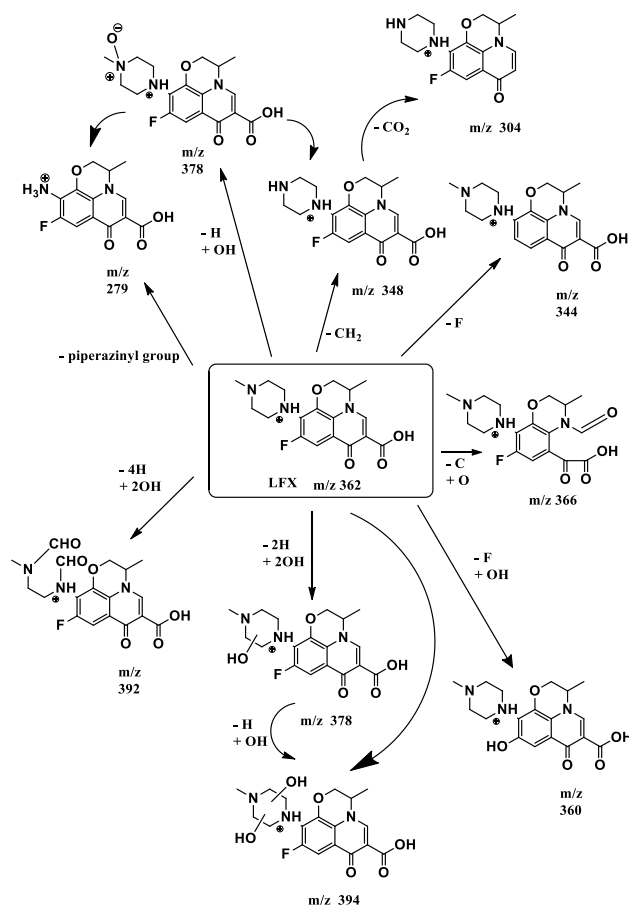


Fig. 5 Possible degradation pathway of LFX in SWW by simulated irradiation/PDS system, after 5 min of irradiation

significant events for LFX degradation mediated by sulphate radicals involving hydroxylation reactions. One of the degradation pathways is associated with the defluorination of LFX.

The intermediate at  $m/z$  344 is due to the neutral loss of fluorine atom in the C-5 position, and, at the same time, the ion at  $m/z$  360 can be obtained by substituting fluorine with OH (Scrano et al. 2020). Previous literature identified the piperazine ring as the most reactive site towards sulphate radicals attack (De Witte et al. 2009; Jiang et al. 2016).

A compound identified at nominal  $m/z$  of 348 exhibited a difference of 14 amu concerning the  $m/z$  ratio of the protonated LFX suggesting the direct formation of de-methylated derivative by loss of a methyl group bonded to N-3, according to previous studies (Jiang et al. 2016; Li et al. 2020). Further neutral loss of  $CO_2$  generates the product at  $m/z$  304, agreeing with Li et al. (2020). The vulnerability of the piperazine group to sulphate radicals attack was confirmed by the other three compounds identified at  $m/z$  378 and 394, and 392. The first two, probably, derived from single and double hydroxylation of piperazine ring, respectively; the third, a

di-aldehyde derivative, due to the cleavage of piperazine ring following the formation of peroxy radicals on two N atoms (Jiang et al. 2016). Because hydroxyl radicals are not selective towards different functional groups, it is impossible to identify the exact position of hydroxylation in the two compounds at  $m/z$  378 and 394. At the same time, based on the fragmentation pathway, retention time, and comparison with the product formed by the addition of PMS, it is possible to attribute the structure of the other compounds identified at  $m/z$  378 to N-oxide levofloxacin (De Witte et al. 2008; Jiang et al. 2016). The direct oxidation of the piperazine side-chain until forming an amino group in position 2 leads to the formation of de-piperazinyl LFX at  $m/z$  279. These by-products define a selective attack of sulphate radicals that induce the piperazine ring opening. In addition, a product with  $m/z$  366 was identified and it was associated with the cleavage of the quinolone moieties instead of the piperazine ring.

## Conclusions

Photon-driven advanced oxidation processes can effectively remove recalcitrant antibacterial pharmaceuticals such as levofloxacin. This work benchmarked the performance of three different precursors of radical oxidant species ( $H_2O_2$ , PMS and PDS) in other pH conditions.

Experiments demonstrated that simulated irradiation/ $H_2O_2$  treatment showed less impact on LFX reduction than the combined AOPs of simulated irradiation/PMS and simulated irradiation/PDS due to the low content of UVC radiation in the solar spectra. In contrast, PMS and PDS were able to degrade levofloxacin completely.

The simulated irradiation/PDS AOP showed the best performance compared to the other oxidation processes evaluated in all mediums investigated, except for phosphate buffer, where PMS resulted in the best. For this medium, exciting results was the complete removal of LFX in 30 s and the formation through the non-radicals mechanism of LFX N-oxide in the presence of PMS. Further studies will focus on product yield quantification to better understand these results.

However, the simulated irradiation/PDS system showed the best performance, achieving a complete degradation of LFX after 10 min of irradiation in all mediums investigated. In simulated wastewater, PDS at different concentrations was tested, and in all cases, the degradation followed a first-order kinetic. Mass balance after treatment indicated that only 125  $\mu$ M PDS was required to attain complete abatement of levofloxacin. However, decreasing the PDS dose may reduce the kinetic rate of levofloxacin abatement. A concentration of 100  $\mu$ M of PDS resulted in optimal removal of LFX in simulated wastewater. The toxicity test allowed inferring that simulated irradiation/PDS can inhibit the antibacterial character of waste effluents, which is relevant to preventing

multi-resistant strains' development. The culture of Gram-positive and Gram-negative bacteria was not affected after the effective degradation of levofloxacin by the sulphate radical-based AOP. Finally, a degradative pathway was suggested from the by-products and intermediates identified by LC-MS. Results demonstrate that the degradation of specific functional groups (i.e., piperazine ring) is associated with the loss of antibacterial character of the molecule. Thus, the mechanism demonstrates the successful degradation of levofloxacin and suggests promising niche application opportunities to ensure pharmaceutical abatement in wastewater effluents. Aromatic by-products were wholly depleted within 10 min of treatment, highlighting simulated irradiation/PDS as a promising technology to mitigate the undesired effects of trace pharmaceuticals pollution in real wastewater effluents.

**Acknowledgements** This work was partially supported by the European Union in the framework of the Project AIM (Attraction and Mobility of Researchers), under the responsibility of the Italian Ministry of University and Research. The authors express their gratitude to the master student, M.L. Palmieri for her collaboration.

**Authors' contributions** Luca Foti: methodology, formal analysis, and writing the original draft. Donatella Coviello: methodology, writing—review and editing. Antonio Zuurro: conceptualization. Filomena Lelario: mass spectrometry data. Sabino Aurelio Bufo: supervision and funding acquisition. Laura Scrano: supervision and funding acquisition. Andres Sauvetre: conceptualization and data acquisition. Serge Chiron: mass spectrometry data and investigation. Monica Brienza: project administration and writing—review and editing.

**Funding** We are grateful to the BIOMON fund, which generously made available materials and instrumental resources.

**Data Availability** Research data can be obtained from the corresponding author through email.

## Declarations

**Ethics approval** This study did not involve human participants, human material, or human data, so it does not need an ethical approval document.

**Consent to participate** Not applicable.

**Consent for publication** All authors have agreed to co-author this manuscript.

**Competing interests** The authors declare that they have no competing interests.

## References

- Ahmed MM, Barbati S, Doumenq P, Chiron S (2012) Sulfate radical anion oxidation of diclofenac and sulfamethoxazole for water decontamination. *Chem Eng J* 197:440–447. <https://doi.org/10.1016/j.cej.2012.05.040>

- Ahmed MM, Brienza M, Goetz V, Chiron S (2014) Solar photo-Fenton using peroxymonosulfate for organic micropollutants removal from domestic wastewater: comparison with heterogeneous TiO<sub>2</sub> photocatalysis. *Chemosphere* 117:256–261. <https://doi.org/10.1016/j.chemosphere.2014.07.046>
- Azzaz AA, Assadi AA, Jellali S, Bouzaza A, Wolbert D, Rtimi S, Bousselmi L (2018) Discoloration of simulated textile effluent in continuous photoreactor using immobilized titanium dioxide: Effect of zinc and sodium chloride. *J Photochem Photobiol A Chem* 358:111–120. <https://doi.org/10.1016/J.JPHOTOCHEM.2018.01.032>
- Backhaus T, Scholze M, Grimme LH (2000) The single substance and mixture toxicity of quinolones to the bioluminescent bacterium *Vibrio fischeri*. *Aquat Toxicol* 49:49–61. [https://doi.org/10.1016/S0166-445X\(99\)00069-7](https://doi.org/10.1016/S0166-445X(99)00069-7)
- Bartlett PD, Cotman JD (1949) The kinetics of the decomposition of potassium persulfate in aqueous solutions of methanol. *J Am Chem Soc* 71:1419–1422. <https://doi.org/10.1021/JA01172A078>
- Boy-Roura M, Mas-Pla J, Petrovic M et al (2018) Towards the understanding of antibiotic occurrence and transport in groundwater: findings from the Baix Fluvià alluvial aquifer (NE Catalonia, Spain). *Sci Total Environ* 612:1387–1406. <https://doi.org/10.1016/j.scitotenv.2017.09.012>
- Brienza M, Katsoyiannis IA (2017) Sulfate Radical Technologies as Tertiary Treatment for the Removal of Emerging Contaminants from Wastewater. *Sustain* 9(9):1604. <https://doi.org/10.3390/SU9091604>
- Brienza M, Mahdi Ahmed M, Escande A, Plantard G, Scrano L, Chiron S, Bufo SA, Goetz V (2014) Relevance of a photo-Fenton like technology based on peroxymonosulphate for 17β-estradiol removal from wastewater. *Chem Eng J* 257:191–199. <https://doi.org/10.1016/J.CEJ.2014.07.061>
- Brienza M, Manasfi R, Chiron S (2019) Relevance of N-nitrosation reactions for secondary amines in nitrate-rich wastewater under UV-C treatment. *Water Res* 162:22–29. <https://doi.org/10.1016/J.WATRES.2019.06.055>
- Brienza M, Manasfi R, Sauvêtre A, Chiron S (2020) Nitric oxide reactivity accounts for N-nitroso-ciprofloxacin formation under nitrate-reducing conditions. *Water Res* 185:116293. <https://doi.org/10.1016/J.WATRES.2020.116293>
- Cai H, Hauser M, Naider F, Becker JM (2016) Halo Assay for Toxic Peptides and Other Compounds in Microorganisms. *Bio-protocol* 6:e2025. <https://doi.org/10.21769/BIOPROT.2025>
- Chu DTW, Fernandest PB (1989) Structure-activity relationships of the fluoroquinolones. *Antimicrob Agents Chemother* 33:131–135. <https://doi.org/10.1128/AAC.33.2.131>
- De Witte B, Dewulf J, Demeestere K et al (2008) Ozonation of ciprofloxacin in water: HRMS identification of reaction products and pathways. *Environ Sci Technol* 42:4889–4895. <https://doi.org/10.1021/es8000689>
- De Witte B, Van LH, Hemelsoet K et al (2009) Levofloxacin ozonation in water: Rate determining process parameters and reaction pathway elucidation. *Chemosphere* 76:683–689. <https://doi.org/10.1016/j.chemosphere.2009.03.048>
- Epold I, Trapido M, Dulova N (2015) Degradation of levofloxacin in aqueous solutions by Fenton, ferrous ion-activated persulfate and combined Fenton/persulfate systems. *Chem Eng J* 279:452–462. <https://doi.org/10.1016/j.cej.2015.05.054>
- Gao Y, Zou D (2020) Efficient degradation of levofloxacin by a microwave-3D ZnCo<sub>2</sub>O<sub>4</sub>/activated persulfate process: Effects, degradation intermediates, and acute toxicity. *Chem Eng J* 393:124795. <https://doi.org/10.1016/j.cej.2020.124795>
- García-Segura S, Nienhauser AB, Fajardo AS, Bansal R, Coonrod CL, Fortner JD, Marcos-Hernandez M, Roders T, Vilagran D, Wong MS, Westerhoff P (2020) Disparities between experimental and environmental conditions: Research steps toward making electrochemical water treatment a reality. *Curr Opin Electrochem* 22:9–16. <https://doi.org/10.1016/J.COEELEC.2020.03.001>
- Geissen V, Mol H, Klumpp E, Umlauf G, Nadal M, Van Der Ploeg M, Van De Zee SEATM, Ritsema CJ (2015) Emerging pollutants in the environment: a challenge for water resource management. *Int Soil Water Conserv Res* 3:57–65. <https://doi.org/10.1016/J.ISWCR.2015.03.002>
- Gothwal R, Shashidhar T (2015) Antibiotic pollution in the environment: a review. *Clean - Soil, Air, Water* 43:479–489. <https://doi.org/10.1002/clen.201300989>
- Hayat W, Zhang Y, Hussain I, Huang S, Du X (2020) Comparison of radical and non-radical activated persulfate systems for the degradation of imidacloprid in water. *Ecotoxicol Environ Saf* 188:109891. <https://doi.org/10.1016/j.ecoenv.2019.109891>
- Jiang C, Ji Y, Shi Y, Chen J, Cai T (2016) Sulfate radical-based oxidation of fluoroquinolone antibiotics: Kinetics, mechanisms and effects of natural water matrices. *Water Res* 106:507–517. <https://doi.org/10.1016/j.watres.2016.10.025>
- Jiménez E, Gilles MK, Ravishankara AR (2003) Kinetics of the reactions of the hydroxyl radical with CH<sub>3</sub>OH and C<sub>2</sub>H<sub>5</sub>OH between 235 and 360 K. *J Photochem Photobiol A Chem* 157:237–245. [https://doi.org/10.1016/S1010-6030\(03\)00073-X](https://doi.org/10.1016/S1010-6030(03)00073-X)
- Jung YJ, Kim WG, Yoon Y, Kang JW, Hong YM, Kim HW (2012) Removal of amoxicillin by UV and UV/H<sub>2</sub>O<sub>2</sub> processes. *Sci Total Environ* 420:160–167. <https://doi.org/10.1016/j.scitotenv.2011.12.011>
- Kamagate M, Assadi AA, Kone T, Giraudet S, Coulibaly L, Hanna K (2018) Use of laterite as a sustainable catalyst for removal of fluoroquinolone antibiotics from contaminated water. *Chemosphere* 195:847–853. <https://doi.org/10.1016/J.CHEMOSPHERE.2017.12.165>
- Kan H, Wang T, Yu J, Qu G, Zhang P, Jia H, Sun H (2021) Remediation of organophosphorus pesticide polluted soil using persulfate oxidation activated by microwave. *J Hazard Mater* 401:123361. <https://doi.org/10.1016/J.JHAZMAT.2020.123361>
- Klein EY, Van Boeckel TP, Martinez EM, Pant S, Gandra S, Levin SA, Goossens H, Laxminarayan R (2018) Global increase and geographic convergence in antibiotic consumption between 2000 and 2015. *Proc Natl Acad Sci* 115:E3463–E3470. <https://doi.org/10.1073/pnas.1717295115>
- Larsson DGJ, de Pedro C, Paxeus N (2007) Effluent from drug manufactures contains extremely high levels of pharmaceuticals. *J Hazard Mater* 148:751–755. <https://doi.org/10.1016/J.JHAZMAT.2007.07.008>
- Lau TK, Chu W, Graham NJD (2007) The aqueous degradation of butylated hydroxyanisole by UV/S<sub>2</sub>O<sub>8</sub><sup>2-</sup>: Study of reaction mechanisms via dimerization and mineralization. *Environ Sci Technol* 41:613–619. <https://doi.org/10.1021/es061395a>
- Lelario F, Brienza M, Bufo SA, Scrano L (2016) Effectiveness of different advanced oxidation processes (AOPs) on the abatement of the model compound mepanipyrin in water. *J Photochem Photobiol A Chem* 321:187–201. <https://doi.org/10.1016/J.JPHOTOCHEM.2016.01.024>
- Li L, Niu CG, Guo H et al (2020) Efficient degradation of Levofloxacin with magnetically separable ZnFe<sub>2</sub>O<sub>4</sub>/NCDs/Ag<sub>2</sub>CO<sub>3</sub> Z-scheme heterojunction photocatalyst: Vis-NIR light response ability and mechanism insight. *Chem Eng J* 383:123192. <https://doi.org/10.1016/j.cej.2019.123192>
- Li Y, Wei D, Du Y (2015) Oxidative transformation of levofloxacin by d-MnO<sub>2</sub>: Products, pathways and toxicity assessment. *Chemosphere* 119:282–288. <https://doi.org/10.1016/j.chemosphere.2014.06.064>
- Liang C, Huang CF, Mohanty N, Kurakalva RM (2008) A rapid spectrophotometric determination of persulfate anion in ISCO. *Chemosphere* 73:1540–1543. <https://doi.org/10.1016/j.chemosphere.2008.08.043>

- Liu B, Li Y, Wu Y, Xing S (2021) Enhanced degradation of ofloxacin by persulfate activation with Mn doped CuO: Synergetic effect between adsorption and non-radical activation. *Chem Eng J* 417:127972. <https://doi.org/10.1016/j.cej.2020.127972>
- Liu X, Fang L, Zhou Y, Zhang T, Shao Y (2013) Comparison of UV/PDS and UV/H<sub>2</sub>O<sub>2</sub> processes for the degradation of atenolol in water. *J Environ Sci* 25:1519–1528. [https://doi.org/10.1016/S1001-0742\(12\)60289-7](https://doi.org/10.1016/S1001-0742(12)60289-7)
- Liu X, Liu Y, Lu S, Wang Z, Wang Y, Zhang G, Guo X, Guo W, Zhang T, Xi B (2020) Degradation difference of ofloxacin and levofloxacin by UV/H<sub>2</sub>O<sub>2</sub> and UV/PS (persulfate): Efficiency, factors and mechanism. *Chem Eng J* 385:123987. <https://doi.org/10.1016/j.cej.2019.123987>
- MacWilliams MP, Liao MK (2006) Luria broth (LB) and Luria agar (LA) media and their uses protocol. ASM MicrobeLibrary Am Soc Microbiol
- Manasfi R, Chiron S, Montemurro N, Perez S, Brienza M (2020) Biodegradation of fluoroquinolone antibiotics and the climbazole fungicide by *Trichoderma* species. *Environ Sci Pollut Res* 27:23331–23341. <https://doi.org/10.1007/s11356-020-08442-8>
- Merel S, Lege S, Yanez Heras JE, Zwiener C (2017) Assessment of N-Oxide Formation during Wastewater Ozonation. *Environ Sci Technol* 51:410–417. <https://doi.org/10.1021/acs.est.6b02373>
- Mukhtar A, Manzoor M, Gul I, Zafar R, Jamil HI, Niazi AK, Ali MA, Park TJ, Arshad M (2020) Phytotoxicity of different antibiotics to rice and stress alleviation upon application of organic amendments. *Chemosphere* 258:127353. <https://doi.org/10.1016/j.CHEMOSPHERE.2020.127353>
- Neth NLK, Carlin CM, Keen OS (2019) Emerging investigator series: Transformation of common antibiotics during water disinfection with chlorine and formation of antibacterially active products. *Environ Sci Water Res Technol* 5:1222–1233. <https://doi.org/10.1039/c9ew00182d>
- Nihemaiti M, Permalá RR, Croué JP (2020) Reactivity of unactivated peroxymonosulfate with nitrogenous compounds. *Water Res* 169:115221. <https://doi.org/10.1016/j.watres.2019.115221>
- Pan LJIA, Li J, Li CX, Tang XD, Yu GW, Wang Y (2018) Study of ciprofloxacin biodegradation by a *Thermus* sp. isolated from pharmaceutical sludge. *J Hazard Mater* 343:59–67. <https://doi.org/10.1016/J.JHAZMAT.2017.09.009>
- Pascale R, Bianco G, Coviello D, Lafiosca MC, Masi S, Mancini IM, Bufo SA, Scrano L, Caniani D (2020) Validation of a liquid chromatography coupled with tandem mass spectrometry method for the determination of drugs in wastewater using a three-phase solvent system. *J Sep Sci* 43:886–895. <https://doi.org/10.1002/jssc.201900509>
- Polo-López MI, García-Fernández I, Velegriaki T, Katsoni A, Oller I, Mantzavinos D, Fernández-Ibáñez P (2012) Mild solar photo-Fenton: An effective tool for the removal of *Fusarium* from simulated municipal effluents. *Appl Catal B Environ* 111–112:545–554. <https://doi.org/10.1016/J.APCATB.2011.11.006>
- Rizzo L, Manaia C, Merlin C, Schwartz T, Dagot C, Ploy MC, Michael I, Fatta-Kassinos D (2013) Urban wastewater treatment plants as hotspots for antibiotic resistant bacteria and genes spread into the environment: A review. *Sci Total Environ* 447:345–360. <https://doi.org/10.1016/j.scitotenv.2013.01.032>
- Scrano L, Foti L, Lelario F (2020) Fluoroquinolones in Water: Removal Attempts by Innovative Aops. In: NATO Science for Peace and Security Series A: Chemistry and Biology. Springer Science and Business Media B.V., pp 259–263
- Serrà A, Philippe L, Perreault F, Garcia-Segura S (2021) Photocatalytic treatment of natural waters. Reality or hype? The case of cyanotoxins remediation. *Water Res* 188:116543. <https://doi.org/10.1016/J.WATRES.2020.116543>
- Shu W, Zhang Y, Wen D, Wu Q, Liu H, Cui M-H, Fu B, Zhang J, Yao Y (2021) Anaerobic biodegradation of levofloxacin by enriched microbial consortia: Effect of electron acceptors and carbon source. *J Hazard Mater* 414:125520. <https://doi.org/10.1016/j.jhazmat.2021.125520>
- Šojić D, Despotović V, Orčić D, Szabò E, Arany E, Armaković S, Illés E, Gajda-Schranz K, Dombi A, Alapi T, Sajben-Nagy E, Palágyi A, Vágvolgyi CS, Manczinger L, Bjelica L, Abramović B (2012) Degradation of thiamethoxam and metoprolol by UV, O<sub>3</sub> and UV/O<sub>3</sub> hybrid processes: Kinetics, degradation intermediates and toxicity. *J Hydrol* 472–473:314–327. <https://doi.org/10.1016/J.JHYDROL.2012.09.038>
- Vagi M, Petsas A (2017) Advanced oxidation processes for the removal of pesticides from wastewater: recent review and trends. 15th Int Conf Environ Sci Technol CEST 2017 31
- Wacławek S, Lutze HV, Grübel K, Padil VVT, Černík M, Dionysiou DD (2017) Chemistry of persulfates in water and wastewater treatment: A review. *Chem Eng J* 330:44–62. <https://doi.org/10.1016/j.cej.2017.07.132>
- Wang J, Wang S (2018) Activation of persulfate (PS) and peroxymonosulfate (PMS) and application for the degradation of emerging contaminants. *Chem Eng J* 334:1502–1517. <https://doi.org/10.1016/j.cej.2017.11.059>
- Wang Q, Wang B, Ma Y, Xing S (2018) Enhanced superoxide radical production for ofloxacin removal via persulfate activation with Cu-Fe oxide. *Chem Eng J* 354:473–480. <https://doi.org/10.1016/j.cej.2018.08.055>
- Yahya MS, El KM, Oturan N, El KK, Oturan MA (2015) Mineralization of the antibiotic levofloxacin in aqueous medium by electro-Fenton process: kinetics and intermediate products analysis. *Environ Technol* 37:1276–1287. <https://doi.org/10.1080/0959330.2015.1111427>
- Yang Q, Ma Y, Chen F, Yao F, Sun J, Wang S, Yi K, Hou L, Li X, Wang D (2019) Recent advances in photo-activated sulfate radical-advanced oxidation process (SR-AOP) for refractory organic pollutants removal in water. *Chem Eng J* 378:122149. <https://doi.org/10.1016/J.CEJ.2019.122149>
- Zainab SM, Junaid M, Xu N, Malik RN (2020) Antibiotics and antibiotic resistant genes (ARGs) in groundwater: A global review on dissemination, sources, interactions, environmental and human health risks. *Water Res* 187:116455. <https://doi.org/10.1016/J.WATRES.2020.116455>
- Zhou Y, Gao Y, Jiang J, Shen YM, Pang SY, Song Y, Guo Q (2021) A comparison study of levofloxacin degradation by peroxymonosulfate and permanganate: Kinetics, products and effect of quinone group. *J Hazard Mater* 403:123834. <https://doi.org/10.1016/j.jhazmat.2020.123834>
- Zhu Y, Zhu R, Xi Y, Zhu J, Zhu G, He H et al (2019) Strategies for enhancing the heterogeneous Fenton catalytic reactivity: A review. *Appl Catal B Environ* 255:117739. <https://doi.org/10.1016/J.APCATB.2019.05.041>
- Zuorro A, Lavecchia R, Monaco MM et al (2019) Photocatalytic Degradation of Azo Dye Reactive Violet 5 on Fe-Doped Titania Catalysts under Visible Light Irradiation. *Catalysts* 9:645. <https://doi.org/10.3390/CATAL9080645>